

Large Porous Particle Impingement on Lung Epithelial Cell Monolayers—Toward Improved Particle Characterization in the Lung

Jennifer Fiegel,^{1,5} Carsten Ehrhardt,^{2,5}
Ulrich Friedrich Schaefer,² Claus-Michael Lehr,² and
Justin Hanes^{1,3,4}

Received October 17, 2002; accepted February 3, 2003

Purpose. The ability to optimize new formulations for pulmonary delivery has been limited by inadequate *in vitro* models used to mimic conditions particles encounter in the lungs. The aim is to develop a physiologically-relevant model of the pulmonary epithelial barrier that would allow for quantitative characterization of therapeutic aerosols *in vitro*.

Methods. Calu-3 human bronchial epithelial cells were cultured on permeable filter inserts under air-interfaced culture (AIC) and liquid-covered culture (LCC) conditions. Calu-3 cells grown under both conditions formed tight monolayers and appeared physiologically similar by SEM and immunocytochemical staining against cell junctional proteins and prosurfactant protein-C.

Results. Aerosolized large porous particles (LPP) deposited homogeneously and reproducibly on the cell surface and caused no apparent damage to cell monolayers by SEM and light microscopy. However, monolayers initially grown under LCC conditions showed a significant decrease in barrier properties within the first 90 min after impingement with microparticles, as determined by transepithelial electrical resistance (TEER) measurements and fluorescein-sodium transport. Conversely, AIC grown monolayers showed no significant change in barrier properties within the first 90 min following particle application. A dense mucus coating was found on AIC grown Calu-3 monolayers, but not on LCC grown monolayers, which may protect the cell surface during particle impinging.

Conclusions. This *in vitro* model, based on AIC grown Calu-3 cells, should allow a more relevant and quantitative characterization of therapeutic aerosol particles intended for delivery to the tracheo-bronchial region of the lung or to the nasal passages. Such characterization is likely to be particularly important with therapeutic aerosol particles designed to provide sustained drug release in the lung.

KEY WORDS: microparticles; pulmonary drug delivery; Calu-3; *in vitro* model.

¹ Department of Chemical & Biomolecular Engineering, The Johns Hopkins University, 3400 N. Charles Street, Baltimore, Maryland 21218.

² Department of Biopharmaceutics and Pharmaceutical Technology, Saarland University, 66123 Saarbrücken, Germany.

³ Department of Biomedical Engineering, The Johns Hopkins University School of Medicine, Baltimore, Maryland 21205.

⁴ To whom correspondence should be addressed. (e-mail: hanes@jhu.edu)

⁵ 1st and 2nd authors contributed equally.

ABBREVIATIONS: LCC, liquid-covered culture; AIC, air-interfaced culture; proSP-C, prosurfactant protein-C; TEER, transepithelial electrical resistance ($\Omega\text{-cm}^2$); flu-Na, fluorescein-sodium; P_{app} , apparent permeability coefficient (cm/s); J, mass flux ($\text{mg}/\text{cm}^2\text{-s}$); A, surface area of permeable membrane (cm^2); C_{donor} , drug concentration in the donor compartment (mg/cm^3); $C_{receptor}$, drug concentration in the receptor compartment (mg/cm^3).

INTRODUCTION

Inhalation of aerosolized drugs holds promise as a means to treat localized disease states within the respiratory tract and may also represent an ideal method for drug delivery to the systemic circulation (1,2). Among non-invasive methods of drug delivery, the respiratory tract offers a more favorable environment compared to the low pH and high protease levels associated with oral delivery. The lung is an attractive route for drug delivery owing to its enormous surface area for absorption ($\sim 100\text{--}140\text{ m}^2$) and permeable epithelium when compared with the gastrointestinal tract (3,4). Although promising, inhalation drug therapy is limited by low particle-delivery efficiencies to the absorptive portion of the lungs (deep lungs or alveolar region) and by the short duration of action of medications in aerosol form (2,5). As a result, most current medical aerosols require inhalation 3–4 times a day to provide desired clinical effects (5).

Large porous particles made with or without a biodegradable polymer have shown considerable promise for achieving sustained drug delivery in the lung (6,7). The ability to optimize these new formulations for pulmonary drug delivery, however, has been limited by a lack of relevant *in vitro* models of the conditions particles encountered in the various regions of the respiratory tract. Conventional “complete immersion” methods used to characterize particle water uptake rates, polymer degradation kinetics, drug diffusion rates, and particle dissolution rates may not be relevant for particles designed for inhalation because of the extremely thin aqueous layers found in the lungs (8,9). These aqueous layers range in depth from approximately $8\ \mu\text{m}$ in the bronchial region to $<0.2\ \mu\text{m}$ in the alveolar region (9), which is one order of magnitude smaller than a typical aerosol particle, and two orders of magnitude smaller than a large porous particle.

An *in vitro* cell culture model that mimics the respiratory epithelium, in particular cells that form tight monolayers and secrete components of mucus or surfactant, would be a valuable tool for microparticle characterization. Calu-3 cells are a human bronchial epithelial cell line isolated from an adenocarcinoma of the lung (10). This cell line has been shown to exhibit serous cell properties and form confluent monolayers of mixed phenotype, including ciliated and secreting cells (11). Recently, the Calu-3 cell line has shown utility as a model to examine the transport (12,13), cellular uptake (14), and metabolism (15) of suspensions or solutions of therapeutics. Calu-3 monolayers were further used to investigate microparticle uptake into the pulmonary epithelium (12), and the protein release, adherence properties, and biocompatibility of protein-loaded polymeric microparticles for nasal delivery (16). However, the effects of culture conditions, specifically liquid-covered culture (LCC) vs. air-interfaced culture (AIC) conditions, and of particle application on the ability of these cells to maintain their barrier properties, have not been examined.

In this study, the authors investigate the influence of culture conditions on the expression of the main proteins related to the cellular junctions and examine the integrity of the Calu-3 cell monolayers impinged with polymeric large porous particles (LPP), by measurement of the transepithelial electrical resistance (TEER) and transport of a paracellular marker (fluorescein-sodium) across the monolayers. These

studies are designed to determine the utility of AIC or LCC grown Calu-3 monolayers as an *in vitro* model to characterize therapeutic aerosol particles. LPP is used as model therapeutic aerosols owing to their promise as carriers for sustained drug release in the lung (6,17).

MATERIALS AND METHODS

Materials

The human adenocarcinoma cell line Calu-3 was obtained from ATCC (Manassas, VA, USA). Mouse IgG1 κ antibody, fluorescein-sodium, tissue culture media, and reagents were all obtained from Sigma (Deisenhofen, Germany). Tissue culture plastics were from Greiner (Frickenhausen, Germany) and Transwell Clear inserts (25.4 mm in diameter, pore size 0.4 μ m) from Corning Costar (Bodenheim, Germany). Rabbit polyclonal ZO-1 antibody was obtained from Zymed (South San Francisco, CA, USA), mouse monoclonal E-cadherin and occludin antibodies were purchased from BD Transduction Laboratories (Heidelberg, Germany) and rabbit polyclonal proSP-C antibody from Chemicon (Hofheim, Germany). FITC-labeled goat anti-mouse F(ab')₂ fragment or swine anti-rabbit F(ab')₂ fragments (both DAKO, Hamburg, Germany) were used as secondary antibodies. Fluor-Save anti-fade medium was obtained from Calbiochem (Bad Soden, Germany). Poly(lactic-co-glycolic acid) with a weight-average molecular weight of 64,000 Daltons was a gift from Alkermes (Medisorb 5050 DL4A, Cincinnati, OH, USA).

Cells and Cell Cultivation

Calu-3 cells of passage number 38 to 56 were seeded onto Transwell Clear permeable filter inserts at a density of 10⁵ cells per cm² (optimal seeding density as determined by TEER measurements and light microscopy). Immediately on seeding, cells were grown in 1500 μ l apical and 2600 μ l basolateral media (Eagle's minimum essential medium supplemented with 10% fetal bovine serum, 0.1 mM nonessential amino acids, 1 mM sodium pyruvate, 100 μ g/ml streptomycin and 100 U/ml penicillin) at 37°C in a 5% CO₂ incubator. The media bathing the cells to be cultured under LCC conditions was removed and cells were fed with 1500 μ l fresh apical and 2600 μ l fresh basolateral media 1 day after seeding and then once daily. The apical medium of cells to be cultured under AIC conditions was removed 1 day after seeding and cells were fed daily with 1400 μ l fresh basolateral media only. Preliminary studies showed no significant influence of coating the filters, either with fibronectin/collagen or Vitrogen-100, on the TEER over 21 days in culture (data not shown).

Immunocytochemical Staining

Rabbit polyclonal ZO-1 antibody, mouse monoclonal occludin antibody, mouse monoclonal E-cadherin IgG1 antibody, and rabbit polyclonal proSP-C antibody were all diluted 1:100 in phosphate-buffered saline (PBS) containing 1% bovine serum albumin (BSA). Mouse IgG1 κ was used as an isotopic control. Cell monolayers were stained 2 weeks after seeding when TEER values peaked (13). Cells were fixed for 10 min with 2% paraformaldehyde and blocked for 10 min in 50 mM NH₄Cl, followed by permeabilization for 8 min with 0.1% Triton X-100. After 60 min incubation with an appro-

prate primary antibody, the monolayers were washed 3 times with PBS before being reacted with a 1:100 dilution of a FITC-labeled goat-anti-mouse F(ab')₂ fragment or swine-anti-rabbit F(ab')₂ fragment in PBS containing 1% BSA. After 30 min incubation, the specimens were washed 3 times with PBS and embedded in FluorSave anti-fade medium. Images were obtained using a confocal laser scanning microscope (MRC-1024, Biorad, München, Germany), with the instrument settings adjusted such that no positive signal was observed in the channel corresponding to green fluorescence of the isotopic controls.

Microparticle Preparation

Poly(lactic-co-glycolic)acid microparticles were made by a double-emulsion solvent-evaporation technique (18). Briefly, 100 μ l of a 10 mg/ml BSA solution was emulsified into a 50 mg/ml polymer solution in methylene chloride by probe sonication (Labsonic 2000, Melsungen, Germany) to form a water-in-oil emulsion. The primary emulsion was poured into 200 ml of an aqueous polyvinyl alcohol solution (average molecular weight 78 kD, 88% hydrolyzed) and homogenized (IKA-Labortechnik, Staufen, Germany) for 1 min to form a double emulsion. The polymeric microparticles were continuously stirred for 2.5 h to allow hardening caused by solvent evaporation, collected by centrifugation, washed 3 times with distilled water, and freeze-dried into a freely-flowing powder. For particle application reproducibility studies, fluorescein-sodium (flu-Na, M_w 376.3 Daltons) was coencapsulated at 75 mg/ml with BSA during microparticle preparation.

Characterization of Polymeric Microparticles

The mass-average size distribution of microparticles was determined using a Coulter Multisizer IIe (Beckman-Coulter Inc., Fullerton, CA, USA). Approximately 2 ml of isoton II solution was added to 5–10 mg microparticles. The solution was briefly vortexed to suspend the microparticles and added dropwise to 100 ml of isoton II solution until the coincidence of particles was between 8% and 10%. Greater than 100,000 particles were sized for each batch of microparticles to determine the mean particle size and size distribution. The bulk density of the particles was determined by tap density as described previously (6).

Microparticle Application on Monolayers

Once cells were grown to confluency (7–8 d after seeding), the apical fluid was removed from the LCC grown Calu-3 monolayers and the basolateral media was reduced to 1400 μ l. AIC grown monolayers were left alone. Filter inserts containing cell monolayers were each transferred from the 6-well plate to a cut-out single well containing prewarmed media. One well was then placed directly under the second stage nozzle of an Astra-type liquid impinger (Erweka, Heusenstamm, Germany) and the impinger was sealed (Fig. 1). Microparticles were aerosolized onto the monolayers for 30 s at 30 L/min from #2 gelatin capsules (Eli Lilly, Indianapolis, IN, USA) using a Spinhaler device (Fisons, Bedford, MA, USA). The filter insert was then returned to the 6-well plate and placed back into an incubator at 37°C.

To obtain data on the reproducibility of the particle application, slightly wetted Transwell Clear filter inserts con-

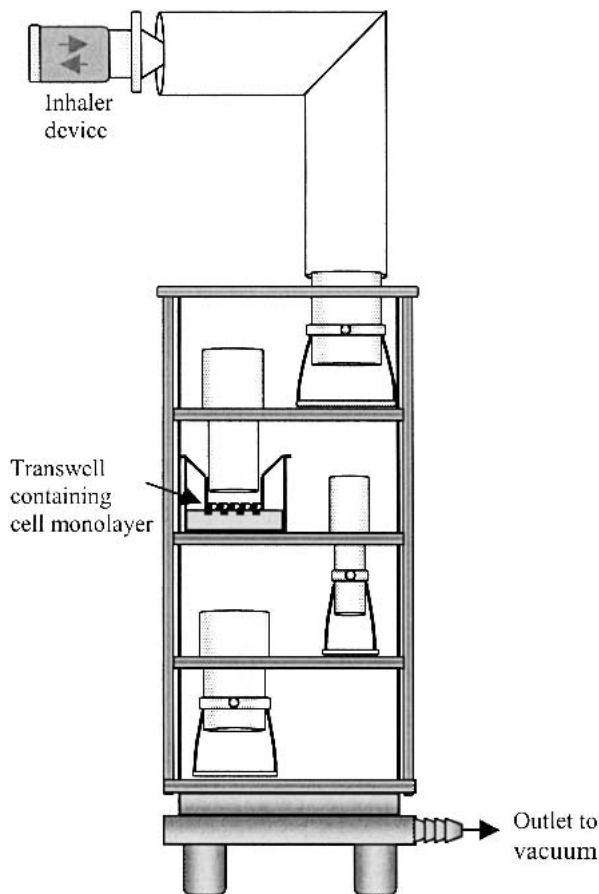


Fig. 1. Diagram of the Astra-type liquid cascade impinger used with a Transwell under the second stage nozzle. Microparticles were aerosolized onto Calu-3 cell monolayers from #2 gelatin capsules using a dry powder inhaler (Spinhaler) and impinger for 30 s at 30 L/min.

taining no cells ($n = 3$) were placed in the impinger and treated as described above. After particle impinging, 0.8 N NaOH was added to the apical and basolateral compartments of the filter to dissolve the microparticles. Following 24 h of incubation at 37°C, the complete degradation of the particles on the filter inserts was verified by light microscopy. Samples were taken and analyzed for flu-Na using a fluorescence plate reader (Cytofluor II, PerSeptive Biosystems, Wiesbaden, Germany) at excitation and emission wavelengths of 485 and 530 nm, respectively. Samples were diluted with KRB where appropriate.

SEM Preparation

Cell monolayers were fixed in glutaraldehyde, critical point dried (CPD030, Bal-Tec, Schalksmühle, Germany) with amyl acetate to remove excess water and mounted onto stubs using double-sided carbon tape. Images were obtained on a Zeiss DSM 940A scanning electron microscope (Göttingen, Germany).

Bioelectric Measurements

To assess the integrity of the cell layer during the transport experiment, the TEER across the monolayers was measured before and after each transport experiment. The long-term effect of microparticle impinging was analyzed by moni-

toring TEER for 1–12 days after application. Experiments were carried out with $n = 6$ filter inserts. TEER was measured with an EVOM device (WPI, Berlin, Germany) equipped with chopstick electrodes. Monolayers grown under LCC conditions were measured directly. Monolayers grown under AIC conditions had 1500 μl and 1200 μl of prewarmed media added to the apical and basolateral sides, respectively, and were allowed to equilibrate for 10 min in an incubator before the TEER measurement was performed. In a second set of experiments, the TEER of cell monolayers was measured immediately following microparticle impingement and after 90 min to assess the short-term effect.

Fluorescein-Sodium Transport across Monolayers

The transport of flu-Na across the cell monolayers was performed immediately after microparticle impinging to determine short-term effects. Experiments were carried out with $n = 3$ using cells from two different passages. After particles were aerosolized onto the cell monolayers, filter inserts were placed into new wells containing 2600 μl of pre-equilibrated bicarbonated Krebs-Ringer solution (KRB, 15 mM HEPES (N-[2-hydroxy-ethyl]piperazine-N'-[2-ethanesulfonic acid]), 116.4 mM NaCl, 5.4 mM KCl, 0.78 mM NaH_2PO_4 , 25 mM NaHCO_3 , 1.8 mM CaCl_2 , 0.81 mM MgSO_4 , 5.55 mM glucose, and pH 7.4) in the basolateral compartment as a receptor solution. Subsequently, 1520 μl of a 50 μM (final concentration) flu-Na solution was added to the apical compartment of each well. The cell monolayers were agitated using an orbital shaker at constant stirring rate (100 rpm) at 37°C under humidified conditions. The initial concentration of flu-Na in the donor fluid was assayed by taking a 20 μl sample. Two hundred microliter-samples were taken at predetermined time points, up to 90 min, from the basolateral compartment (receptor) and replaced with an equal amount of fresh buffer. The fluorescence of flu-Na was measured in 96-well plates using a fluorescence plate reader (Cytofluor II, PerSeptive Biosystems, Wiesbaden, Germany) at excitation and emission wavelengths of 485 and 530 nm, respectively. Samples were diluted with KRB where appropriate.

The flu-Na flux across the monolayers (J) was determined by plotting cumulative amounts of drug transported across the cell layer vs. time. Apparent permeability coefficients of the cell monolayers, P_{app} , were calculated from steady state transport data according to Fick's first law:

$$J = P_{app} \cdot A \cdot (C_{donor} - C_{receptor}) \quad (1)$$

where C_{donor} is the concentration in the donor compartment (apical side), $C_{receptor}$ is the concentration in the receptor compartment (basolateral side), and A is the surface area of the filter used in this study.

Light Microscopy

After two weeks in culture, Calu-3 cell monolayers grown under LCC and AIC conditions were washed with PBS, fixed in Bouin's solution and dehydrated in 2-propanol. Cells were then stained with nuclear fast red, eosin Y, aniline blue and orange G to show nuclei and acidic glycoproteins typically found in mucus. Images were obtained on a Zeiss Axiovert 100 microscope (Göttingen, Germany).

Statistical Analysis

Results are expressed as mean \pm S.E.M. Significant ($p < 0.05$) differences in the TEER and P_{app} values from several ($n \geq 3$) data groups were determined by one-way analysis of variances (ANOVA), followed by Neumann–Keuls–Student post-hoc tests.

RESULTS

Immunocytochemical Staining

The expression profiles of junctional proteins, ZO-1, occludin, and E-cadherin in Calu-3 cell monolayers grown on permeable membrane inserts (Fig. 1) under LCC and AIC conditions were assessed by immunocytochemical staining. The expression profile for tight junctional proteins, ZO-1 and occludin, showed a regular appearance along the intercellular interface in both LCC (Fig. 2, left panel) and AIC (Fig. 2, right panel) grown Calu-3 cell monolayers. A regular staining pattern along the cell-cell interface was also observed for those of the adherens junction protein, E-cadherin, in both AIC and LCC grown monolayers. Similarly, both LCC and AIC grown Calu-3 monolayers exhibited bright punctate staining profiles for proSP-C (Fig. 2).

Characterization of Polymeric Microparticles

The mass-mean size of polymeric microparticles used in this study was 9.9 μm , with a GSD of 1.4, each determined using a Coulter Multisizer. The GSD was determined from (19):

$$\text{GSD} = \frac{d_{84\%}}{d_{50\%}} \quad (2)$$

where d_n is the diameter at the n th percentile of the cumulative distribution. The microparticle bulk density, as determined by tap density measurements, was 0.43 g/ml. The mass-median aerodynamic diameter (d_a), the in-flight diameter a spherical particle would possess assuming it had a density of 1 g/ml, was 6.5 μm as found from the relationship:

$$d_a = \frac{d}{\gamma} \sqrt{\rho/\rho_a} \quad (3)$$

where d = geometric diameter, γ = shape factor = 1 for a sphere, ρ = particle mass density (g/ml), and ρ_a = water mass density (1 g/ml). This aerodynamic diameter was appropriate for aerosolization onto the 2nd stage of the liquid impinger used in this study.

Large Porous Particle (LPP) Aerosolization on Calu-3 Cell Monolayers

Polymeric LPPs were aerosolized from a dry powder inhaler onto the Calu-3 monolayers located under the second stage nozzle of a liquid impinger (Fig. 1). LPPs were homogeneously dispersed as single particles on the cell monolayers, as observed using light microscopy (Fig. 3a). No apparent damage to the cell monolayers was observed using light microscopy and scanning electron microscopy (SEM). SEM images showed particles on monolayers with visually tight intercellular borders (Fig. 3b and 3c). Formation of microvilli was apparent on the apical plasma membranes of Calu-3 cells by

SEM (Fig. 3b). A broken microparticle shows the high porosity of the LPPs (Fig. 3c). LPP aerosolization reproducibility studies using blank filters showed that $192 \pm 12 \mu\text{g}$ of flu-Na loaded microparticles was administered per filter insert ($n = 4$).

Effects of Microparticle Application on Cell Monolayers

Before microparticle application, both AIC and LCC grown Calu-3 monolayers exhibited a steady increase in trans-epithelial electrical resistance (TEER) during the first week of culture, with monolayers maintained under LCC conditions exhibiting a significantly ($p < 0.05$) higher TEER value than AIC grown monolayers (Fig. 4). From day 8 onward, the TEER of all AIC grown monolayers remained approximately constant at a mean value of $700 \Omega\text{-cm}^2$, whether they were impinged with microparticles, air, or nothing (Fig. 4). On the other hand, LCC grown monolayers experienced a significant drop in TEER on the day of impingement on removal of the apical media prior to impingement (day 7), even in the absence of particle impingement onto the cell monolayers (Fig. 4). After day 13, the TEER of LCC grown monolayers remained approximately constant at a mean value of $700 \Omega\text{-cm}^2$. Therefore, both culture conditions resulted in a similar long-term resistance. It is important to note that TEER values were not measured for 1–3 days after impinging in this experiment. Therefore, additional studies were performed immediately after microparticle application to determine any short-term effects of the impinging process on the integrity of the cell monolayers.

In this second set of experiments, the transport of fluorescein-sodium (flu-Na) across the cell monolayers was performed for 90 min immediately following microparticle impingement. Monolayers grown under LCC conditions exhibited a significant increase in flu-Na flux following microparticle deposition compared to the control (no impingement) and air-impinged monolayers (Fig. 5). The increase in flux resulted from an increase in the monolayer permeability (Table I), and correlated to a decrease in TEER of approximately $1600 \Omega\text{-cm}^2$ compared to the control (Fig. 6A). In contrast, monolayers grown under AIC exhibited no significant change in flu-Na flux (Fig. 5), P_{app} (Table I) or TEER values (Fig. 6B) following air or microparticle impingement compared to the control.

The P_{app} of the cell monolayers to flu-Na was calculated using Eq. 1 for the linear region of the flu-Na transport curves (Table I). AIC and LCC grown monolayers that were neither air nor LPP impinged displayed similar P_{app} values of 2.2×10^{-7} and 2.3×10^{-7} cm/sec, respectively. In addition, AIC grown monolayers exhibited similar P_{app} values, regardless of the impingement process. Air impingement onto the LCC grown monolayers caused the P_{app} value to approximately double to 4.8×10^{-7} cm/sec, and microparticle impingement caused a significantly larger increase in P_{app} , to 11.5×10^{-7} cm/sec. After a short lag period (the time needed to reach a steady state flux), the P_{app} across the monolayers impinged with microparticles maintained a near constant value.

Light Microscopy

Calu-3 monolayers grown under LCC and AIC conditions exhibited a cobblestone morphology (Fig. 3b) typical for

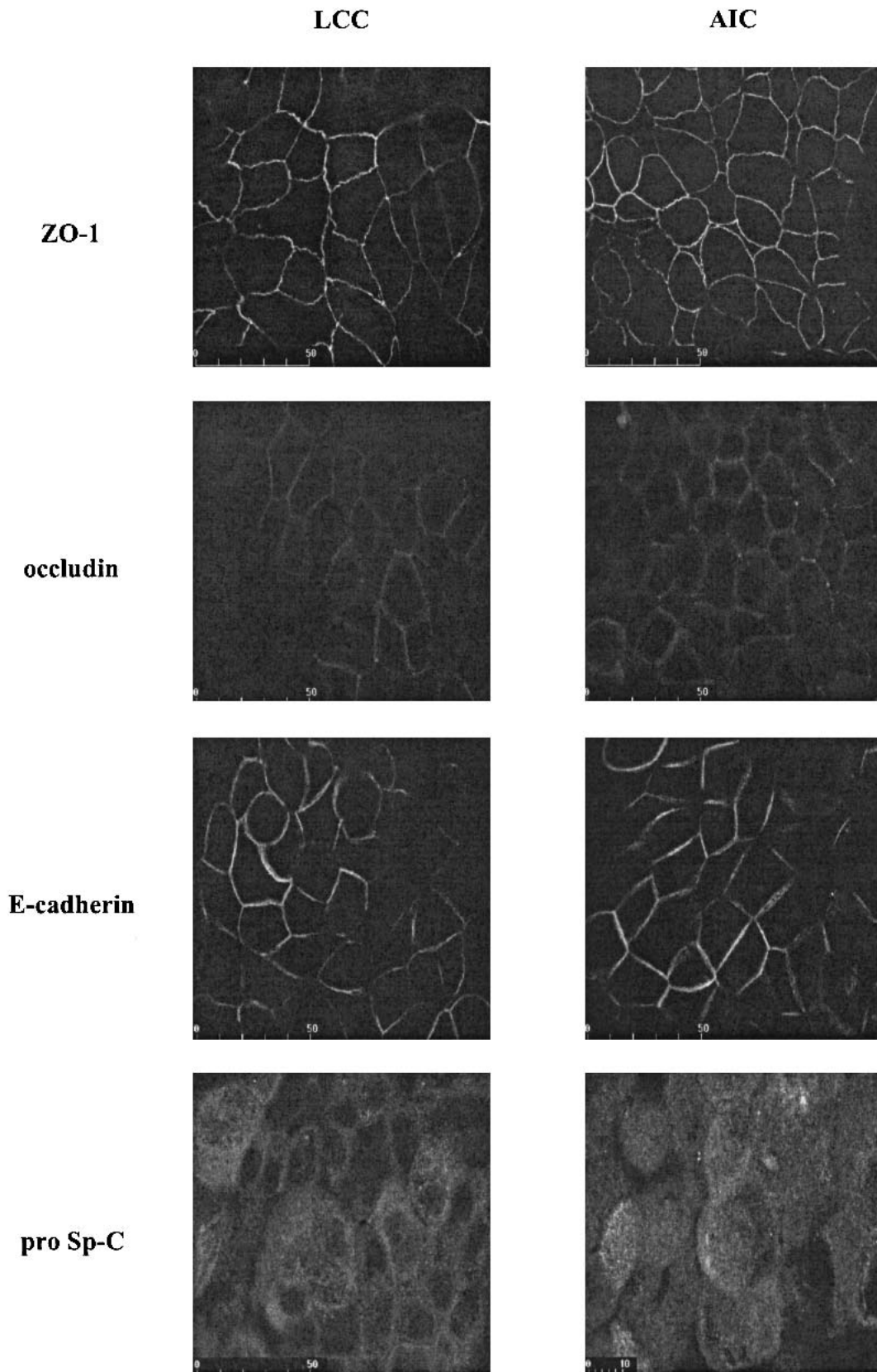


Fig. 2. Expression profiles of ZO-1, occludin, E-cadherin, and proSP-C in Calu-3 cells. Cells were seeded at a density of 10^5 cells per cm^2 on Transwell Clear inserts and cultured under LCC (left panel) conditions throughout, or AIC conditions from day 1 onward (right panel). Cultured cell layers were stained after 2 wk in culture for ZO-1 (top panel), occludin (second panel), E-cadherin (third panel) and proSP-C (bottom panel) as described. Scale bars represent μm .

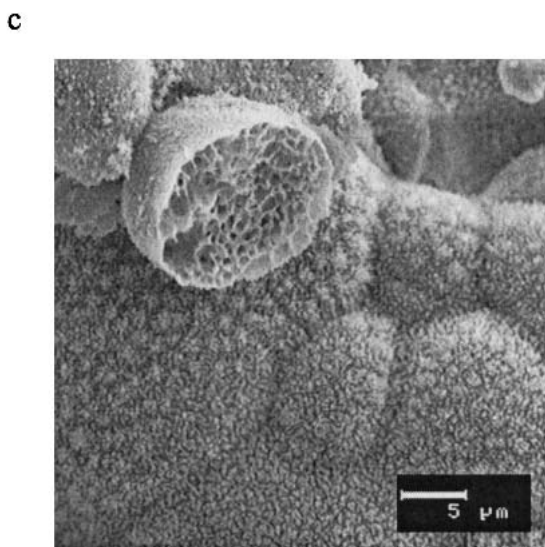
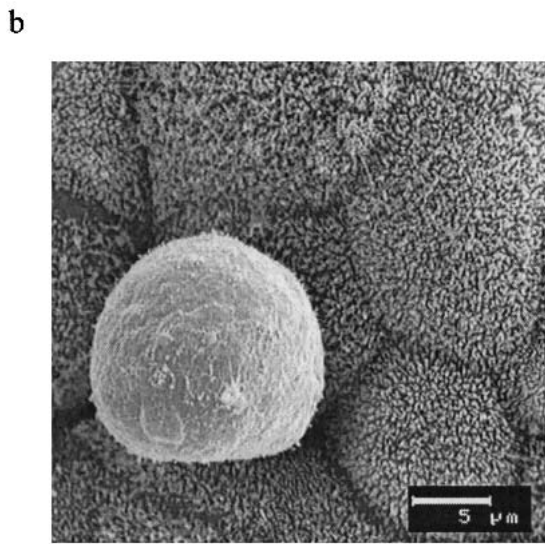
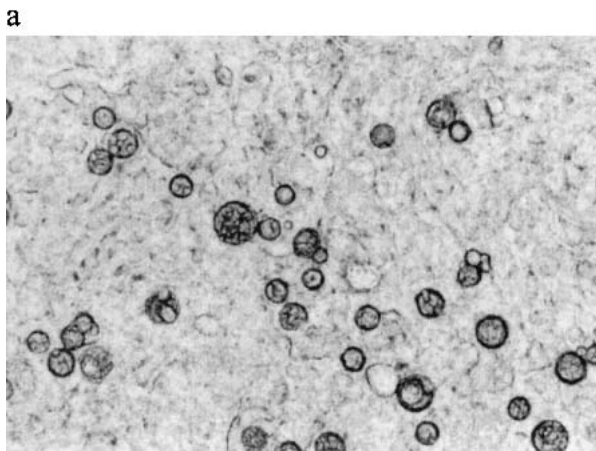


Fig. 3. (a) Inverted microscope image showing microparticles homogeneously distributed on *Calu-3* cell monolayers following aerosolization, magnification $\times 400$. Scanning electron microscopy images showing (b) a polymeric particle on top of a Transwell Clear grown *Calu-3* cell monolayer and (c) the high internal porosity of a typical large porous particle. Cell layers were impinged after 8 days in culture and fixed for EM as described.

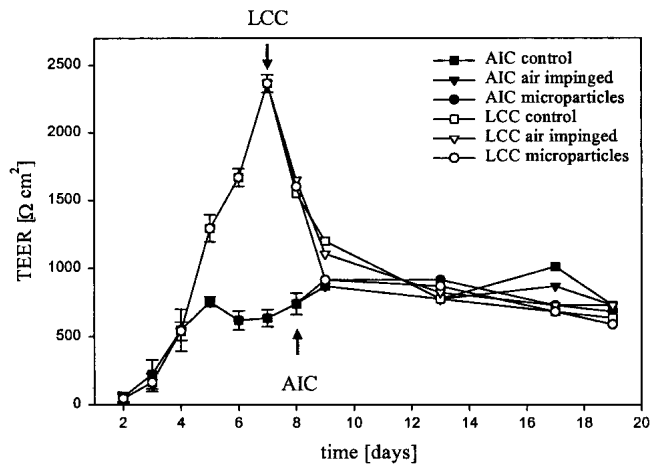


Fig. 4. Time course of TEER development in *Calu-3* cell monolayers. Cells were seeded at a density of 10^5 cells per cm^2 on Transwell Clear inserts and cultured under LCC conditions throughout, or under AIC conditions from day 1 onward. The monolayers were impinged with particles after one week of culture (arrows) and kept under AIC conditions thereafter (Mean \pm SD, N = 6).

airway epithelial cells. Cells were stained with eosin Y, aniline blue and orange G to show acidic glycoproteins typically found in mucus. No evidence of mucus could be found on LCC grown monolayers, whereas monolayers grown under AIC conditions showed strong staining on the entire cell surface (Fig. 7).

DISCUSSION

Current *in vitro* methods for the characterization of aerosol particles generally rely on complete immersion in physiologic buffers. Immersion methods allow easy particle separation from the immersion solution, allowing quantification of properties such as particle dissolution and/or polymer degradation and drug release from polymeric particles. However, therapeutic aerosols delivered to the respiratory system land

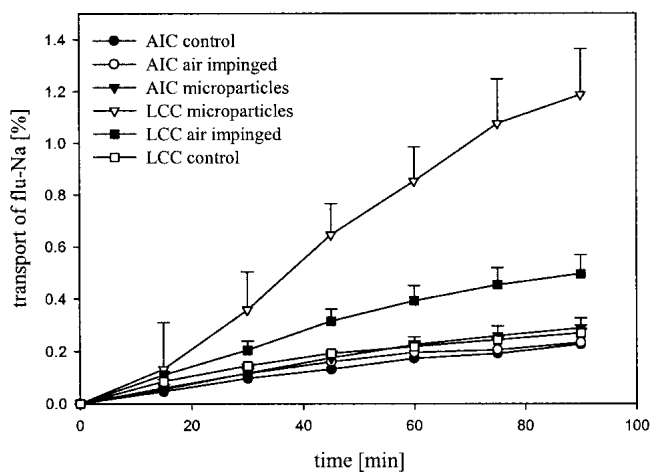


Fig. 5. Transport rates of fluorescein-sodium across *Calu-3* cell monolayers. Cells were seeded at a density of 10^5 cells per cm^2 on Transwell Clear inserts and cultured under LCC conditions throughout, or under AIC conditions from day 1 onward. The monolayers were impinged with microparticles or air after one week of culture (Mean \pm S.E.M., N = 6).

Table I. P_{app} [$\times 10^{-7}$ cm/sec] Values \pm S.E.M. of Fluorescein Sodium across Untreated Calu-3 Monolayers (Control), Calu-3 Monolayers Impinged with Air (Air Impinged), and with Microparticles

	Culture conditions	P_{app} ($\times 10^{-7}$ cm/sec)
Control	AIC (n = 5)	2.2 ± 0.4
	LCC (n = 8)	2.2 ± 0.2
Air impinged	AIC (n = 8)	2.3 ± 0.5
	LCC (n = 8)	4.9 ± 0.7
Microparticles	AIC (n = 8)	2.9 ± 0.4
	LCC (n = 7)	11.8 ± 3.1

on thin aqueous layers of mucus or surfactant lining airway epithelial cells. Therefore, the development of a physiologically-relevant model to characterize aerosol particles was needed.

In vitro cell line and primary cell culture models of the respiratory epithelium have been developed to predict important *in vivo* biologic phenomena, including drug transport (13,20–22). Compared to cell lines, primary cell culture models have the disadvantage of being derived from heterogeneous sources and exhibit both an acute phenotypic instability and lack of longevity in culture (23). Cell line models of the

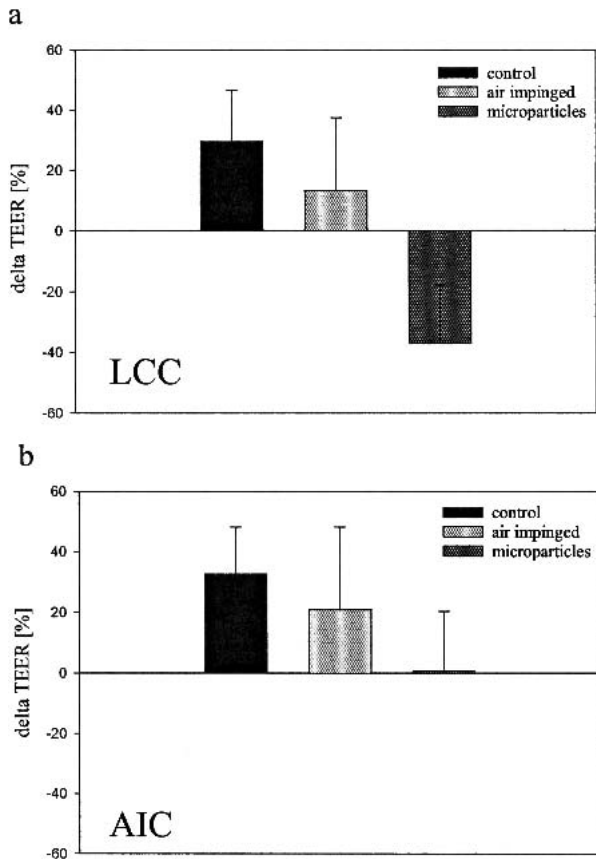


Fig. 6. Change in transepithelial electrical resistance (TEER) of Calu-3 cell monolayers following microparticle impinging by way of aerosolization. Cells were seeded at a density of 10^5 cells per cm^2 on Transwell Clear inserts and cultured under (a) LCC conditions throughout or under (b) AIC conditions from day 1 onward. Microparticles were aerosolized onto the monolayers after one week of culture and the change in TEER after microparticle impinging was assessed (Mean \pm S.E.M., N = 6).

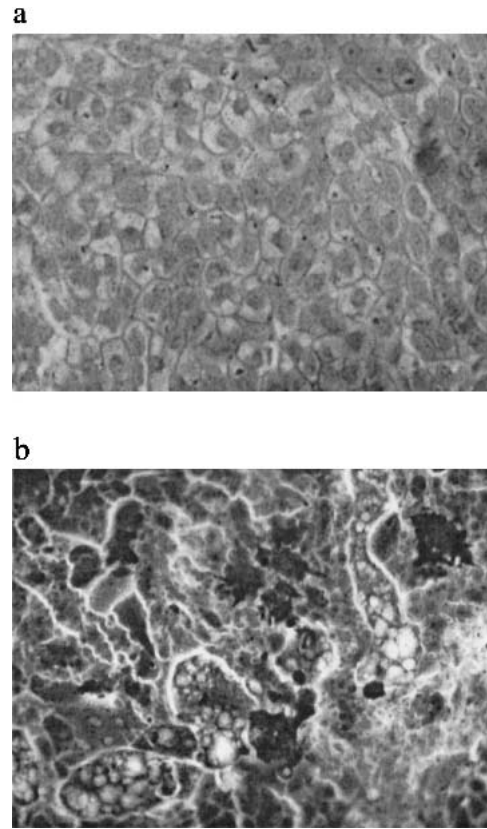


Fig. 7. Light photomicrograph of Calu-3 cells after two weeks in culture. Cells were seeded at a density of 10^5 cells per cm^2 on Transwell Clear inserts and (a) cultured under LCC throughout or (b) AIC conditions from day 1 onward. Cells were stained as described. Cell borders and nuclei are apparent in (a), but the cell monolayer is covered by mucus in (b). Magnification $\times 400$.

pulmonary epithelium, however, often lack one or more potentially important features, such as intercellular junctions, expression of certain receptors, and physiologic levels of product secretion found in healthy *in vivo* tissues (23,27). Therefore, to successfully mimic a biologic barrier with an *in vitro* cell culture system, the selection of the cell line is particularly important.

A recent publication focused on 16HBE14o-human bronchial epithelial cells used in combination with a glass impinger to mimic the nasal target site (24). However, the 16HBE14o-cell line may not be an appropriate model for studies at an air-interface, because of its reported inability to form tight intracellular junctions when cultured under AIC conditions (20). In our studies, the Calu-3 cell line was chosen as the model barrier for their ability to form tight monolayers of pulmonary cells and to secrete components of mucus and surfactant.

Calu-3 cells grown and maintained under LCC conditions achieve much higher TEER values than cells grown under AIC conditions. However, primary cultures of human airway epithelia often exhibit markedly improved differentiation when cultured under AIC conditions (22,25), with a few notable exceptions (20,26). No conclusive evidence that either culture condition produces cell monolayers that are more similar to *in vivo* lung epithelial tissue has been reported. Therefore, to determine differences between Calu-3 cells

grown under AIC and LCC conditions, the authors investigated the influence of culture conditions on the expression of the main proteins of cellular junctions.

Information on the influence of culture conditions on formation of cellular junctions is important for the characterization of an *in vitro* model for drug absorption, because the tight junctions constitute the principal barrier to passive movement of fluid, electrolytes, and macromolecules through the paracellular pathway (27). Proteins that are involved in the formation of tight junctions include the transmembrane proteins, occludins and claudins, and the intracellular proteins ZO-1, ZO-2 and ZO-3. Formation of the tight junctions in epithelia is also known to be accompanied by that of zonula adherens. Located at the zonula adherens is the type I membrane protein, E-cadherin, that connects neighboring cells by Ca^{2+} -dependent interactions. Alterations in the organization of tight junctions that influence the paracellular permeability of the epithelial cell layers can be studied by measuring transepithelial electrical resistance (TEER), or the permeability of the cell monolayer to a paracellularly transported marker substance. A decrease in TEER below a threshold value (28) generally corresponds with an increase in paracellular permeability.

In the current study, junctional protein staining showed that the AIC and LCC grown monolayers appear to be physiologically similar prior to microparticle application. Both culture conditions led to tight monolayers that expressed tight junction and adherens junction proteins between the cell borders. In addition, both AIC and LCC conditions produced cell monolayers that express the lung surfactant-specific protein proSP-C on the cellular surface, proving the cells retain at least part of their lung-specific function. Bronchial epithelial cells *in vivo* are covered by a mucus lining that protects the surface against a constant assault from airborne particles. The mucus is composed primarily of glycoproteins, water, and a thin surfactant layer. Surfactant protein C (Sp-C) is one of four surfactant-specific proteins commonly found in the surfactant fluid. Due to its hydrophobic nature, it seems to be important in determining the surface properties of pulmonary surfactant (29).

To assess the paracellular permeability of Calu-3 cells, transport experiments were performed on consecutive days in culture. The P_{app} value of flu-Na decreased with increasing transepithelial electrical resistance and reached a plateau at TEER values higher than $\sim 450 \Omega\text{-cm}^2$ for both AIC and LCC conditions (13). Again, no differences between cell monolayers grown under AIC and LCC conditions were identified.

Our intent, however, was to apply aerosol particles under "dry" conditions (by way of a dry powder inhaler) without causing a disruption in Calu-3 monolayer properties relevant to particle characterization and drug transport. Because neither culture condition could be eliminated based on junctional staining or permeability, monolayers grown under each culture condition were examined after impinging with microparticles to determine their suitability in particle characterization studies.

Light microscopy images of the monolayers confirmed that particles were not aggregated when seeded on the monolayers and were dispersed homogeneously across the entire membrane (e.g. particles did not concentrate at the walls or in the center) (Fig. 3a). Application of PLGA microparticles encapsulating flu-Na onto blank filters resulted in reproduc-

ible particle deposition. Light microscopy and SEM images of both AIC and LCC grown monolayers seeded with particles, showed tight monolayers with no apparent damage to the monolayers (Fig. 3).

Although the P_{app} vs. TEER data (13) suggested that experiments could be performed on monolayers with TEER values greater than $450 \Omega\text{-cm}^2$, the authors chose to use monolayers once they had reached a steady TEER value so that they could easily isolate the effects of microparticle application from the effects of monolayer growth on TEER. At the time of microparticle impingement, monolayers grown under LCC conditions showed an increase in flux of the paracellular marker, caused by increase in monolayer permeability, when compared to the controls. This suggested a reversible decrease of the barrier properties of the LCC grown monolayers. The TEER of the monolayers grown under LCC conditions always dropped on removal of the apical fluid prior to particle impingement, but TEER decrease was significantly enhanced by microparticle impingement onto the cell surface (Fig. 6). A few days after impinging with particles, LCC grown monolayers recovered from the impinging process and remained at a steady TEER value for at least 9 days. The initial period, however, is critical for characterization of drug transport. As a result, cell monolayers grown under LCC conditions were deemed unsuitable for particle characterization studies involving measurement of drug transport.

On the other hand, monolayers grown under AIC conditions showed no change in Flu-Na flux, P_{app} , or TEER following particle impinging, indicating no change in barrier properties. In addition, monolayers reached a steady TEER value ($\sim 700 \Omega\text{-cm}^2$) that was approximately the same as that for the LCC grown monolayers after impinging. This value is above that necessary for tight monolayers with Calu-3 cells, as monolayers with TEER values $\geq 450 \Omega\text{-cm}^2$ exhibit identical permeability toward low molecular weight substances, such as flu-Na (13,28).

Mucus staining of the cell monolayers showed positive staining only for Calu-3 cells grown under AIC conditions. The mucus on monolayers grown under AIC conditions may protect cell barrier properties on microparticle impingement by providing a protective coating, cushioning the landing of the particles. On the other hand, mucus produced by cells grown under LCC conditions likely dissolves into the apical fluid as it is produced, and is removed on aspiration prior to particle impinging. The absence of the mucosal barrier exposes the apical cell surface. Therefore, microparticles landing directly on the surface of cells grown under LCC conditions may cause short-term damage to their barrier properties, leading to the increased flux of the paracellular marker found in these studies. Because Calu-3 cells grown under AIC conditions exhibit a uniform mucus layer on their apical surface, quantitative characterization of aerosols intended for delivery to the tracheo-bronchial region of the lung or to the nasal passages utilizing these cell monolayers should be more physiologically relevant than traditional submersion characterization. A limitation of this model, that is shared with other cell culture models of the tracheo-bronchial region of the lung, is the absence of mucociliary clearance.

In conclusion, Calu-3 cells cultured under air-interfaced conditions provide an appropriate surface (tight monolayers that secrete components of mucus and surfactant) for the characterization of aerosol particles. Future work will focus

on the use of this *in vitro* characterization tool to study water uptake rates, particle degradation and dissolution kinetics, and drug transport through the particles and cell monolayers.

ACKNOWLEDGMENTS

This research was supported by the Whitaker Foundation (JH and JF, DGE-9616062), the National Science Foundation (JH and JF, RG-99-0046) and the ZEBET (CE, UFS and CML, WK 1-1328-152). The authors thank Steffen Dillinger (Dept. of Zoology and Bionics, Saarland University) for assistance in obtaining the scanning electron micrographs.

REFERENCES

1. J. S. Patton and R. Platz. Pulmonary delivery of peptides and proteins for systemic action. *Adv. Drug Deliv. Rev.* **8**:179–196 (1992).
2. S. Sanjar and S. Matthews. Treating systemic diseases via the lung. *J. Aerosol Med.* **14**:S51–S58 (2001).
3. J. S. Patton. Inhalation: The other “oral” route for delivery of molecules with low gastrointestinal bioavailability. *Abstr. Pap. Am. Chem. Soc.* **219**:175 (2000).
4. R. W. Niven. Delivery of biotherapeutics by inhalation aerosol. *Crit. Rev. Ther. Drug Carrier Syst.* **12**:151–231 (1995).
5. X. M. Zeng, G. P. Martin, and C. Marriott. The controlled delivery of drugs to the lung. *Int. J. Pharm.* **124**:149–164 (1995).
6. D. A. Edwards, J. Hanes, G. Caponetti, J. Hrkach, A. Ben-Jebria, M. L. Eskew, J. Mintzes, D. Deaver, N. Lotan, and R. Langer. Large porous particles for pulmonary drug delivery. *Science* **276**:1868–1871 (1997).
7. R. Vanbever, A. Ben-Jebria, J. D. Mintzes, R. Langer, and D. A. Edwards. Sustained release of insulin from insoluble inhaled particles. *Drug Dev. Res.* **48**:178–185 (1999).
8. E. R. Weibel. *Morphometry of the Human Lung*, Academic Press, New York, 1963.
9. J. Bastacky, C. Y. Lee, J. Goerke, H. Koushafar, D. Yager, L. Kenaga, T. P. Speed, Y. Chen, and J. A. Clements. Alveolar lining layer is thin and continuous: low-temperature scanning electron microscopy of rat lung. *J. Appl. Physiol.* **79**:1615–1628 (1995).
10. J. Fogh and G. Trempe. In J. Fogh (ed.), *Human Tumor Cells In Vitro*, Plenum Press, New York, 1975 pp. 115–159.
11. B. Q. Shen, W. E. Finkbeiner, J. J. Wine, R. J. Mrsny, and J. H. Widdicombe. Calu-3: a human airway epithelial cell line that shows cAMP-dependent Cl⁻ secretion. *Am. J. Physiol.* **266**:L493–L501 (1994).
12. K. A. Foster, M. Yazdaniyan, and K. L. Audus. Microparticulate uptake mechanisms of in-vitro cell culture models of the respiratory epithelium. *J. Pharm. Pharmacol.* **53**:57–66 (2001).
13. J. Moebius, C. Ehrhardt, I. Erler, U. F. Schaefer, and C. M. Lehr. The epithelial cancer cell line Calu-3: Characterization as an in vitro model for drug absorption in the upper airways. *Arch. Pharm. Pharm. Med. Chem.* **333**:13 (2001).
14. M. E. Cavet, M. West, and N. L. Simmons. Transepithelial transport of the fluoroquinolone ciprofloxacin by human airway epithelial Calu-3 cells. *Antimicrob. Agents. Ch.* **41**:2693–2698 (1997).
15. B. I. Florea, I. C. van der Sandt, S. M. Schrier, K. Kooiman, K. Deryckere, A. G. de Boer, H. E. Junginger, and G. Borchard. Evidence of P-glycoprotein mediated apical to basolateral transport of flunisolide in human broncho-tracheal epithelial cells (Calu-3). *Br. J. Pharmacol.* **134**:1555–1563 (2001).
16. C. Witschi and R. J. Mrsny. In vitro evaluation of microparticles and polymer gels for use as nasal platforms for protein delivery. *Pharm. Res.* **16**:382–390 (1999).
17. J. Fu, J. Fiegel, E. Krauland, and J. Hanes. New polymer carriers for controlled drug delivery following inhalation or injection. *Biomaterials* **23**:4425–4433 (2002).
18. J. Hanes, D. A. Edwards, C. Evora, and R. Langer. Particles incorporating surfactants for pulmonary drug delivery. U.S. Patent No. 5,855,913 (1999).
19. W. C. Hinds. *Aerosol Technology—Properties, Behavior, and Measurement of Airborne Particles*, John Wiley & Sons, Inc., New York, 1999.
20. C. Ehrhardt, C. Kneuer, J. Fiegel, J. Hanes, U. F. Schaefer, K. J. Kim, and C. M. Lehr. Influence of apical fluid volume on the development of functional intercellular junctions in the human epithelial cell line 16HBE14o-: implications for the use of this cell line as an in vitro model for bronchial drug absorption studies. *Cell Tissue Res.* **308**:391–400 (2002).
21. K. J. Elbert, U. F. Schaefer, H. J. Schafers, K. J. Kim, V. H. L. Lee, and C. M. Lehr. Monolayers of human alveolar epithelial cells in primary culture for pulmonary absorption and transport studies. *Pharm. Res.* **16**:601–608 (1999).
22. M. Yamaya, W. E. Finkbeiner, S. Y. Chun, and J. H. Widdicombe. Differentiated structure and function of cultures from human tracheal epithelium. *Am. J. Physiol.* **262**:L713–L724 (1992).
23. H. Wan, H. L. Winton, C. Soeller, G. A. Stewart, P. J. Thompson, D. C. Gruenert, M. B. Cannell, D. R. Garrod, and C. Robinson. Tight junction properties of the immortalized human bronchial epithelial cell lines Calu-3 and 16HBE14o-. *Eur. Respir. J.* **15**:1058–1068 (2000).
24. B. Forbes, S. Lim, G. P. Martin, and M. B. Brown. An in vitro technique for evaluating inhaled nasal delivery systems. *S.T.P. Pharma.* **12**:75–79 (2002).
25. M. Kondo, W. E. Finkbeiner, and J. H. Widdicombe. Cultures of bovine tracheal epithelium with differentiated ultrastructure and ion transport. *In Vitro Cell. Dev. Biol.* **29A**:19–24 (1993).
26. P. M. de Jong, M. A. J. A. van Sterkenburg, J. A. Kempenaar, J. H. Dijkman, and M. Ponc. Serial culturing of human bronchial epithelial cells derived from biopsies. *In Vitro Cell. Dev. Biol.* **29A**:379–387 (1993).
27. K. J. Kim, Z. Borok, and E. D. Crandall. A useful in vitro model for transport studies of alveolar epithelial barrier. *Pharm. Res.* **18**:253–255 (2001).
28. C. Ehrhardt, J. Fiegel, S. Fuchs, R. Abu-Dahab, U. F. Schaefer, J. Hanes, and C. M. Lehr. Drug absorption by the respiratory mucosa - cell culture models and particulate drug carriers. *J. Aerosol Med.* **15**:131–139 (2002).
29. L. Cruewels, L. Golde, and H. Haagsman. The pulmonary surfactant system: Biochemical and clinical aspects. *Lung* **175**:1–39 (1997).